JACS
JOURNAL OF THE AMERICAN CHEMICAL SOCIETY
Article
pubs.acs.org/JACS

α/β-Peptide Foldamers Targeting Intracellular Protein–Protein Interactions with Activity in Living Cells

James W. Checco,[†] Erinna F. Lee,[‡,§,#] Marco Evangelista,[‡,#] Nerida J. Sleebs,[‡] Kelly Rogers,[‡,§] Anne Pettikiriarachchi,[‡] Nadia J. Kershaw,[‡,§] Geoffrey A. Eddinger,[†] David G. Belair,[⊥] Julia L. Wilson,[†] Chelcie H. Eller,[∥] Ronald T. Raines,[†,∥] William L. Murphy,[⊥,▽] Brian J. Smith,[◆] Samuel H. Gellman,*[,†] and W. Douglas Fairlie*[,‡,§,#]

[†]Department of Chemistry, [⊥]Department of Biomedical Engineering, [∥]Department of Biochemistry, and [▽]Department of Orthopedics and Rehabilitation, University of Wisconsin-Madison, Madison, Wisconsin 53706, United States

[‡]The Walter and Eliza Hall Institute of Medical Research, Parkville, Victoria 3052, Australia

[§]Department of Medical Biology, University of Melbourne, Parkville, Victoria 3010, Australia

[◆]Department of Chemistry and Physics, La Trobe Institute of Molecular Science, Melbourne, Victoria 3086, Australia

Supporting Information

ABSTRACT: Peptides can be developed as effective antagonists of protein–protein interactions, but conventional peptides (i.e., oligomers of L-α-amino acids) suffer from significant limitations *in vivo*. Short half-lives due to rapid proteolytic degradation and an inability to cross cell membranes often preclude biological applications of peptides. Oligomers that contain both α- and β-amino acid residues ("α/β-peptides") manifest decreased susceptibility to proteolytic degradation, and when properly designed these unnatural oligomers can mimic the protein-recognition properties of analogous "α-peptides". This report documents an extension of the α/β-peptide approach to target intracellular protein–protein interactions. Specifically, we have generated α/β-peptides based on a "stapled" Bim BH3 α-peptide, which contains a hydrocarbon cross-link to enhance α-helix stability. We show that a stapled α/β-peptide can structurally and functionally mimic the parent stapled α-peptide in its ability to enter certain types of cells and block protein–protein interactions associated with apoptotic signaling. However, the α/β-peptide is nearly 100-fold more resistant to proteolysis than is the parent stapled α-peptide. These results show that backbone modification, a strategy that has received relatively little attention in terms of peptide engineering for biomedical applications, can be combined with more commonly deployed peripheral modifications such as side chain cross-linking to produce synergistic benefits.

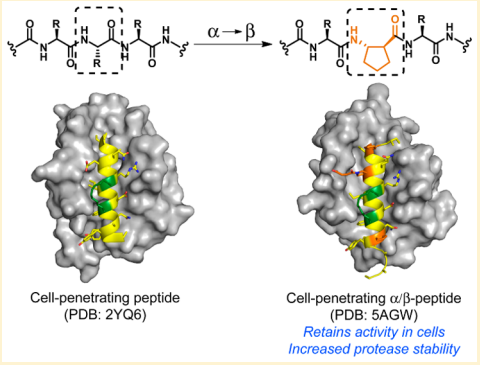

INTRODUCTION

Misregulation of protein–protein interactions is often associated with disease states, and compounds that selectively modulate such interactions may be used as therapeutic agents. Small molecules, the traditional choice for drug compounds, are often ineffective at targeting protein–protein interactions because of the large protein contact surfaces involved in many of these associations.[1] In contrast, medium-length peptides can be developed to bind with high affinity and selectivity to large surfaces on proteins. However, *in vivo* applications of peptides are often severely limited because of their rapid degradation by proteolytic enzymes.[2] Furthermore, because most peptides do not spontaneously cross cell membranes, intracellular protein–protein interactions are typically not viable targets for peptide antagonists.

Oligomers that contain both α- and β-amino acid residues ("α/β-peptides") can mimic natural α-helices and modulate helix-mediated protein–protein interactions.[3,4] The unnatural backbone of the α/β-peptide reduces susceptibility to protease degradation relative to peptides that consist only of α-amino acid residues ("α-peptides").[5] Our prior work has shown that α/β-peptides can function as antagonists in cell-based systems.[4,6,7] Recently, we reported that α/β-peptides can also show prolonged activity *in vivo* relative to the parent α-peptides, highlighting the potential of these compounds for therapeutic use.[8] To date, the design of biologically active α/β-peptides has been limited to protein–protein interactions that occur at the cell surface.

α-Helical secondary structures play an important role in many protein–protein interactions.[9] We have previously used α-helical BH3 domains from Bcl-2 family proteins as a model system for exploring the effects of α → β-amino acid residue substitutions on the recognition of a helical ligand by partner proteins.[3,10,11] BH3 domains are short (~20-residues) α-helical segments that mediate interactions between pro- and anti-

Received: June 7, 2015
Published: August 28, 2015

DOI: 10.1021/jacs.5b05896
J. Am. Chem. Soc. 2015, 137, 11365–11375

apoptotic Bcl-2 family proteins.[12] These domains bind to long, complementary grooves displayed by anti-apoptotic family members such as Bcl-x_L, Mcl-1, and Bcl-2. Binding of members of the BH3-only subclass (e.g., Bim, Puma, Bad) to anti-apoptotic partners results in the initiation of apoptosis in damaged, redundant, or potentially dangerous cells. These interactions displace pro-apoptotic proteins such as Bax, Bak, or "activator" BH3-only proteins from sequestration by the anti-apoptotic family members. This release of pro-apoptotic factors triggers mitochondrial membrane permeabilization, cytochrome *c* release, and caspase activation. The survival versus death decision is finely controlled by the balance of pro- and anti-apoptotic Bcl-2 family members within a cell. Several types of cancer cells rely on overexpression of certain anti-apoptotic Bcl-2 family proteins as a mechanism to evade cell death. This observation has engendered speculation that antagonism of anti-apoptotic Bcl-2 family proteins could be beneficial for cancer treatment.[13] Indeed, several small molecule Bcl-2 family protein antagonists have recently shown promising results in cancer patient samples and clinical trials.[14]

Other groups have sought to improve the properties of short peptides similar to BH3 domain-derived α-peptides by introducing side chain cross-links that are intended to stabilize the binding conformation (an α-helix). A variety of different strategies have been employed,[17] including lactam cross-linking via amino acid residue side chains,[18,19] alkylation of cysteine residues with cross-linking groups,[20] and alkene cross-linking using olefin metathesis.[21] Use of a hydrocarbon cross-link, formed by ring-closing metathesis of two α,α-disubstituted pentenyl-containing amino acids (S5) at *i* and *i* + 4 positions (e.g., ***α*-1**, Figure 1), has been the most intensively studied strategy.[15,16,22−24] These "stapled" α-helical ("SAH") peptides display increased helicity and decreased susceptibility to protease action relative to conventional α-peptide analogues.

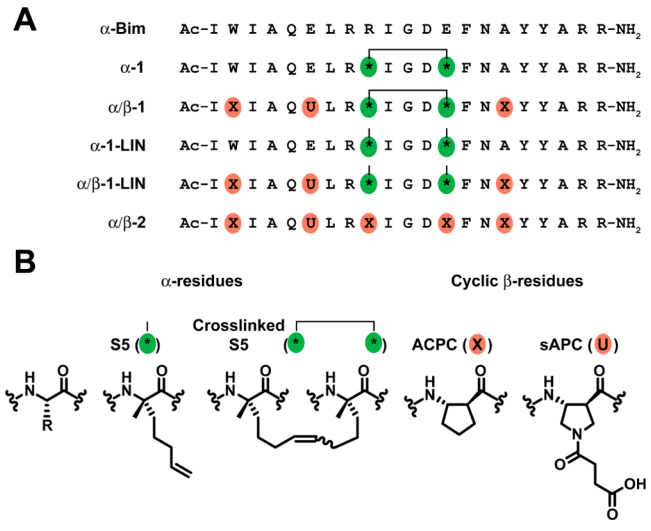

Figure 1. (A) Primary sequences of α- and α/β-peptides used in this study. The cross-linked α-peptide ***α*-1** has been referred to as **BimSAHB** in prior reports.[15,16] Non-natural amino acid residues are indicated by colored circles: green for S5 residue used for cross-linking, and orange for cyclic β-residues. A horizontal line connecting two S5 residues indicates that these residues have been cross-linked using olefin metathesis. (B) Structures of a generic α-residue, the S5 residue (*), two cross-linked S5 residues, and the cyclic β-residues ACPC (X) and sAPC (U).

In some exceptional cases the stapled peptide manifests cellular permeability that is not observed for related α-peptides containing only natural residues. The mechanism for cellular entry of stapled helical peptides is not understood, but it has been suggested that the hydrophobic cross-linker allows association of the peptide with the cellular membrane, with subsequent cell entry proceeding via energy-dependent endocytosis.[23] Some stapled analogues of BH3 domains that enter cells can initiate apoptosis by antagonizing the actions of anti-apoptotic Bcl-2 proteins.[16,23]

Here we describe α/β-peptide analogues of ***α*-1** (previously reported in the literature as **BimSAHB**),[15,16] a cross-linked α-helical α-peptide derived from the Bim BH3 domain. The "stapled" α/β-peptide mimics the activity of the cross-linked parent α-peptide in cell-based experiments. However, the cross-linked α/β-peptide manifests greater resistance to proteolytic degradation than does the analogous cross-linked α-peptide. These results show that properly designed α/β-peptides can recapitulate favorable characteristics of stapled peptides, such as protein recognition, conformational stability, and membrane permeability, while providing additional benefits. Such compounds may be useful as chemical probes for studying interactions among Bcl-2 family proteins within cells or as starting points for the development of future therapeutic agents.

RESULTS

Design of *α*/*β*-Peptide Mimics of *α*-1. We recently reported α/β-peptide analogues of the Bim BH3 domain that contain cyclic β-amino acid residues (ACPC and sAPC, Figure 1B) and bind to both Bcl-x_L and Mcl-1 with high affinity.[11] These α/β-peptides are significantly less susceptible to proteolytic degradation relative to α/β-peptides that contain only flexible, acyclic β-residues. Based on this precedent, we designed ***α*/*β*-1** (Figure 1), an analogue of ***α*-1** that contains three $\alpha \rightarrow$ cyclic β-residue substitutions (Trp2 → ACPC, Glu6 → sAPC, Ala16 → ACPC) along with the side chain cross-link. We also synthesized linear "unstapled" analogues of ***α*-1** and ***α*/*β*-1** (***α*-1-LIN** and ***α*/*β*-1-LIN**, respectively) to evaluate the effect of the covalent cross-link on protein affinity and cellular activity. As a further basis of comparison, we prepared ***α*/*β*-2**, an analogue of ***α*/*β*-1-LIN** that contains two hydrophobic ACPC cyclic β-residues in place of the S5 residues.

Protein Binding by SPR. We used a surface plasmon resonance (SPR) competition assay to evaluate the affinity of the Bim-derived α- and α/β-peptides to three key anti-apoptotic proteins: Bcl-x_L, Mcl-1, and Bcl-2 (Table 1). ***α*-1**, ***α*/*β*-1**, ***α*-1-LIN**, and ***α*/*β*-1-LIN** all bound to Mcl-1 as tightly as did the parent ***α*-Bim** sequence. ***α*/*β*-1** also bound to Bcl-x_L and Bcl-2 similarly to ***α*-Bim**, while ***α*-1**, ***α*-1-LIN**, and ***α*/*β*-1-LIN** generally bound one or both of these anti-apoptotic proteins somewhat more weakly than did ***α*-Bim** (up to ∼50-fold decline in affinity, depending on the combination). Interestingly, ***α*/*β*-2**, an analogue of ***α*/*β*-1-LIN** that contains the cyclic β-residue ACPC in place of the S5 residues, retained relatively high affinity for Mcl-1 but displayed reduced affinity for Bcl-x_L and Bcl-2 compared to ***α*/*β*-1-LIN**. Overall, these data imply that ***α*/*β*-1** mimics the protein recognition profiles of both ***α*-Bim** and ***α*-1**, which suggests that the incorporation of cyclic β-amino acid residues into this sequence, in place of α-residues, does not negatively impact the affinity for anti-apoptotic proteins. Indeed, for some anti-apoptotic proteins,

DOI: 10.1021/jacs.5b05896
J. Am. Chem. Soc. 2015, 137, 11365−11375

Table 1. Binding to Anti-Apoptotic Proteins by SPR and Proteolysis Data for α- and α/β-Peptides

	IC_{50} (nM) [SPR][a]			
oligomer	Bcl-x_L	Mcl-1	Bcl-2	$t_{1/2}$ (min)[b]
α-Bim	4.1 (0.5)	4.4 (0.4)	3.6 (0.6)	0.27
α-1	22.2 (4.8)	3.3 (0.4)	66.6 (13.6)	1.6
α/β-1	4.5 (3.4)	4.1 (2.9)	10.2 (1.4)	150
α-1-LIN	80.0 (7.5)	4.0 (0.2)	189 (33)	–
α/β-1-LIN	5.5 (0.8)	4.0 (0.5)	50.5 (10.1)	–
α/β-2	579 (202)	15.7 (5.6)	1323 (234)	–

[a]Relative binding of oligomers to anti-apoptotic proteins determined by competition SPR assays, based on 2–5 independent experiments. Numbers in parentheses indicate standard deviation. [b]Half-life of 40 μM α- or α/β-peptide in the presence of 10 μg/mL proteinase K in TBS, pH 7.5 with 8% DMSO. Dashes indicate that the oligomer was not tested in the assay.

the interaction with **α/β-1** is stronger than the interaction with **α-1**.

Structural Analysis in Solution by Circular Dichroism. To gain insight into the impact of the hydrocarbon cross-link on oligomer conformation in solution, we examined the far-UV circular dichroism (CD) spectra of Bim-derived α- and α/β-peptides (Figure 2). Consistent with previous reports,[15,16] **α-Bim** showed little evidence of helicity in aqueous solution, while the stapled peptide **α-1** showed a strong α-helical signature in the far-UV CD, with minima at ~208 and 222 nm. Interestingly, **α-1-LIN**, the "unstapled" analogue of **α-1**, also showed a pronounced α-helical CD signature, although the minima were less intense than those of **α-1**. This result suggests that incorporation of the α,α-disubstituted S5 residue alone is sufficient to promote a helical conformation, although not to the extent observed with an intact cross-link. **α/β-1** and **α/β-1-LIN** both showed a single minimum at ~209 nm, consistent with the signal observed for α/β-peptides that adopt an α-helix-like conformation in solution.[25] As seen for the **α-1-LIN** versus **α-1** comparison, **α/β-1-LIN** displayed a less intense helical signature relative to cyclized analogue **α/β-1**. We note that the CD signal intensity for all of the peptides containing the S5 residue, with or without cyclization, was concentration dependent in the range of 5–50 μM (Figure S2), which suggests that these peptides aggregate under these conditions. Hence, the relative differences in the signal intensities for the linear versus cross-linked peptides could reflect slightly altered propensities to aggregate rather than differences in helix stability.

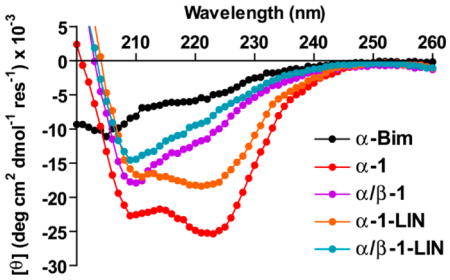

Figure 2. Far-UV CD spectra of α- and α/β-peptides at 50 μM in water at 20 °C.

Crystal Structures of α/β-1 and α/β-1-LIN in Complex with Bcl-2. To gain atomic-resolution insight regarding the impact of the β-amino acid residues and the hydrocarbon cross-link on binding to an anti-apoptotic protein partner, we solved X-ray crystal structures of **α/β-1** (PDB: 5AGW) and **α/β-1-LIN** (PDB: 5AGX) in complex with Bcl-2 (Figure 3, Table S1).

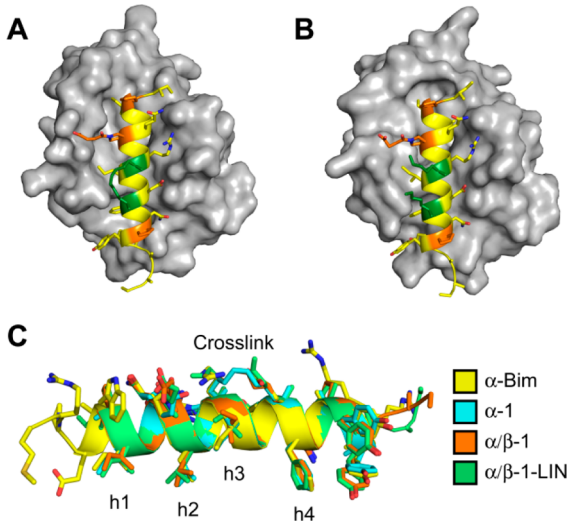

Figure 3. Crystal structures of α/β-peptides **α/β-1** and **α/β-1-LIN** bound to Bcl-2. (A) Structure of **α/β-1** bound to Bcl-2 (PDB: 5AGW). (B) Structure of **α/β-1-LIN** bound to Bcl-2 (PDB: 5AGX). In A and B, the α/β-peptide is colored by residue type (yellow for natural α-residues, green for S5 residues, and orange for cyclic β-residues) and the Bcl-2 surface is shown in gray. (C) Overlay of **α/β-1** and **α/β-1-LIN** with previously reported structures of an analogue of **α-Bim** (bound to Bcl-x_L, PDB: 3FDL)[26] and an analogue of **α-1** (bound to Bcl-x_L, PDB: 2YQ6).[19] Positions of key protein-contacting hydrophobic residues h1–h4 and the position of the cross-link (for **α-1** and **α/β-1**) are labeled.

The two α/β-peptides crystallized with Bcl-2 under similar conditions and produced similar crystal forms. No structure is available for the **α-Bim**:Bcl-2 complex for comparison, but both **α/β-1** and **α/β-1-LIN** engage Bcl-2 via the large hydrophobic groove (formed by helices α3, α4, and the N-terminal segment of α5) that is known to be the interaction site on Bcl-2 for BH3 peptide ligands (Figure 3A,B); comparable grooves are evident in structures of other anti-apoptotic proteins.[26−29] The four conserved hydrophobic residues (h1–h4) on the buried face of the α/β-peptides project into the groove on Bcl-2 in a manner similar to that in which equivalent residues on **α-Bim** and **α-1** interact with the equivalent groove on Bcl-x_L (Figure 3C). The salt bridge between Asp12 of the α/β-peptides and Arg146 from the BH1 domain of Bcl-2 matches a salt-bridge observed in most reported structures of BH3 domains bound to anti-apoptotic proteins. As anticipated, the β-amino acid residues of **α/β-1** and **α/β-1-LIN** are aligned as a "stripe" along the solvent-exposed face of the helix formed by each α/β-peptide. In the **α/β-1**:Bcl-2 complex structure the long sAPC side chain from **α/β-1** projects close to the α3 helix of Bcl-2 and may form a hydrogen bond to the side chain of Glu114 if at least one of the carboxyl groups is protonated. The hydrocarbon cross-link in the **α/β-1**:Bcl-2 complex overlays almost perfectly with the cross-link in the structure of **α-1** bound to Bcl-x_L (PDB: 2YQ6).[19] Neither cross-link makes any contacts with the anti-apoptotic protein. In the **α/β-1-LIN**:Bcl-2 complex structure the S5 side chains project out to the solvent.

DOI: 10.1021/jacs.5b05896
J. Am. Chem. Soc. 2015, 137, 11365–11375

Cytochrome *c* Release Assay (Permeabilized Cells). To establish whether ***α/β*-1** could neutralize anti-apoptotic protein function in a cellular milieu, we tested whether this stapled *α/β*-peptide could induce cytochrome *c* release from mitochondria (a hallmark of cell death induction). These studies were conducted in wild-type mouse embryonic fibroblasts (MEFs) in which the plasma membrane was permeabilized by treatment with digitonin (Figure 4). This permeabilization approach is

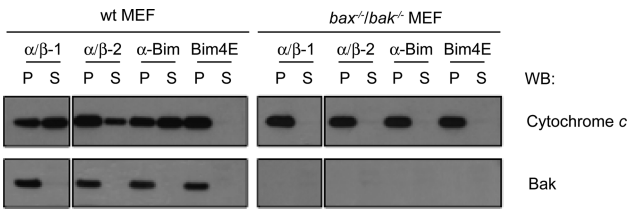

Figure 4. Cytochrome *c* release assay on permeabilized wild-type (wt) or $bax^{-/-}/bak^{-/-}$ mouse embryonic fibroblasts (MEFs) treated with 10 μM of the indicated *α*- or *α/β*-peptide for 1 h. ***α/β*-1**, ***α/β*-2**, and ***α*-Bim** were able to induce cytochrome *c* release from the mitochondria-containing pellet fraction (P) to the soluble cytosolic fraction (S) in wt MEFs, but not in $bax^{-/-}/bak^{-/-}$ MEFs, as indicated by Western blot for cytochrome *c*. No cytochrome *c* release was seen for negative control **Bim4E** (DMRPEIWEAQEERREGDEENAYYARR-OH). The lower panel shows Western blot for Bak as a control for membrane permeabilization. Bak is a mitochondrial protein and therefore should not appear in the cytosolic fraction. The $bax^{-/-}/bak^{-/-}$ MEFs do not have Bak, and therefore no band is apparent. Irrelevant intervening lanes between ***α/β*-1** and ***α/β*-2** have been cropped from the image.

usually required to enable BH3-derived peptides to reach the proteins that regulate apoptosis.[10,11] Mouse embryonic fibroblasts express both Bcl-x_L and Mcl-1, and both proteins contribute to MEF cell survival.[30] Hence, BH3 peptides must antagonize both Bcl-x_L and Mcl-1 to induce apoptosis. Consistent with its binding profile for these anti-apoptotic proteins, ***α/β*-1** induced movement of cytochrome *c* from the pellet fraction (which contains the mitochondria) to the soluble cytosolic fraction in permeabilized MEFs. Comparable behavior was observed with the ***α*-Bim** peptide, which is comprised solely of *α*-residues (Figure 4). Slightly less cytochrome *c* release was observed with ***α/β*-2** relative to ***α/β*-1**, consistent with the difference in affinity for Bcl-x_L between these two *α/β*-peptides (Table 1). No cytochrome *c* release was seen with a negative control Bim-derived *α*-peptide (**Bim4E**) in which key interacting residues (h1−h4) were mutated to glutamic acid, or in permeabilized MEFs derived from embryos deficient in Bax and Bak, the essential mediators of apoptosis. Combined, these data suggest that ***α/β*-1** can neutralize Bcl-x_L and Mcl-1 in permeabilized cells, leading to the activation of Bax and/or Bak.

Cell Killing Assays. Previous studies have shown that some cell types, particularly hematological cancer cell lines, are either killed or are sensitized to apoptosis by treatment with stapled BH3 domain *α*-peptides, but that other cell lines (e.g., fibroblasts, HCT-116 colon cancer) are resistant to these stapled peptides.[16,19,23,31] We therefore screened a panel of various cell lines to identify those cells that could be used in detailed functional analyses. The cross-linked *α/β*-peptide ***α/β*-1** was compared to the cross-linked *α*-peptide ***α*-1** at a high concentration (10 μM) in a CellTiter-Glo assay (Promega), which measures intracellular ATP levels as an indicator of cell viability (Figure 5). Consistent with previous reports for ***α*-1**,[16] we saw essentially no effect of ***α/β*-1** or ***α*-1** on MEFs (Figure

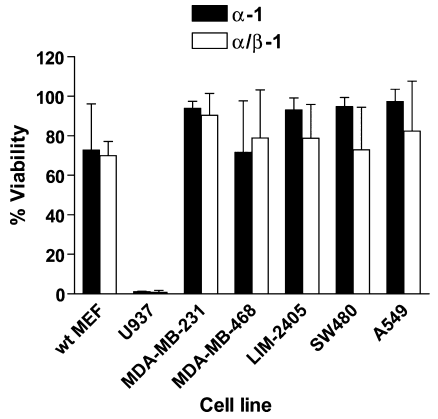

Figure 5. Viability of various cell lines (relative to DMSO control) when exposed to 10 μM ***α*-1** (black bars) or ***α/β*-1** (white bars) for 24 h, as measured using CellTiter-Glo assay. Each bar represents the mean ± SD for two independent experiments.

5), which are not cancer cells, even though ***α/β*-1** can engage the apoptotic network when the MEF outer membrane has been permeabilized (Figure 4). Additionally, no significant cell death was induced by ***α/β*-1** or ***α*-1** with any of the adherent cancer cell lines tested, including those derived from mammary (MDA-MB-231, MDA-MB-468), colon (LIM-2405, SW480), or lung (A549) tumors. In contrast, ***α/β*-1** potently impacted U937 lymphoma cell viability, similar to the effect previously observed with ***α*-1** on these cells.[16] Overall, these data indicate that ***α/β*-1** mimics the highly selective cell-killing profile of ***α*-1**, suggesting that the non-natural *α/β* backbone supports mimicry of the complex biological activity of the stapled *α*-peptide ***α*-1**.

To gain insight into the relative potency of ***α/β*-1** versus ***α*-1** toward U937 cells and to establish whether the loss of cell viability observed following treatment was due to activation of the apoptotic cascade or to some nonspecific effect (e.g., rupture of the plasma membrane), we performed titrations of ***α*-1** or ***α/β*-1** in the presence or absence of the broad-spectrum caspase inhibitor Q-VD-OPh (Figure 6). Following just 2 h of treatment with cross-linked oligomer in the absence of caspase inhibitor, a significant reduction in cell viability was observed for cells treated with either ***α*-1** or ***α/β*-1**. This loss in viability was attenuated by Q-VD-OPh for both the stapled *α*-peptide and the stapled *α/β*-peptide, suggesting that the cell killing was due to activation of the intrinsic cell death pathways (in which caspases play a critical role) rather than a nonspecific effect. Additional caspase-dependent killing was seen after 6 h of treatment for both oligomers; however, after treatment with peptides for 24 h, most of the cell death observed was not inhibited by Q-VD-OPh. ***α*-1** was slightly more potent than ***α/β*-1** (EC_{50} = ∼2 μM for ***α*-1** versus ∼4 μM for ***α/β*-1** at 6 h), but there appeared to be slightly more caspase-independent killing (not blocked by Q-VD-OPh) at the earlier time points for ***α*-1** compared to ***α/β*-1**.

Recent reports[31,32] suggest that the hydrocarbon cross-link per se may not be required for cell entry of some stapled peptides, but rather that the presence of the two S5 residues alone (no cyclization via ring-closing metathesis) may be sufficient to facilitate cell entry and initiation of apoptosis. To evaluate the importance of the hydrocarbon cross-link in our system, we tested the linear peptides ***α*-1-LIN** and ***α/β*-1-LIN** for killing activity toward U937 cells. Consistent with an earlier

DOI: 10.1021/jacs.5b05896
J. Am. Chem. Soc. 2015, 137, 11365−11375

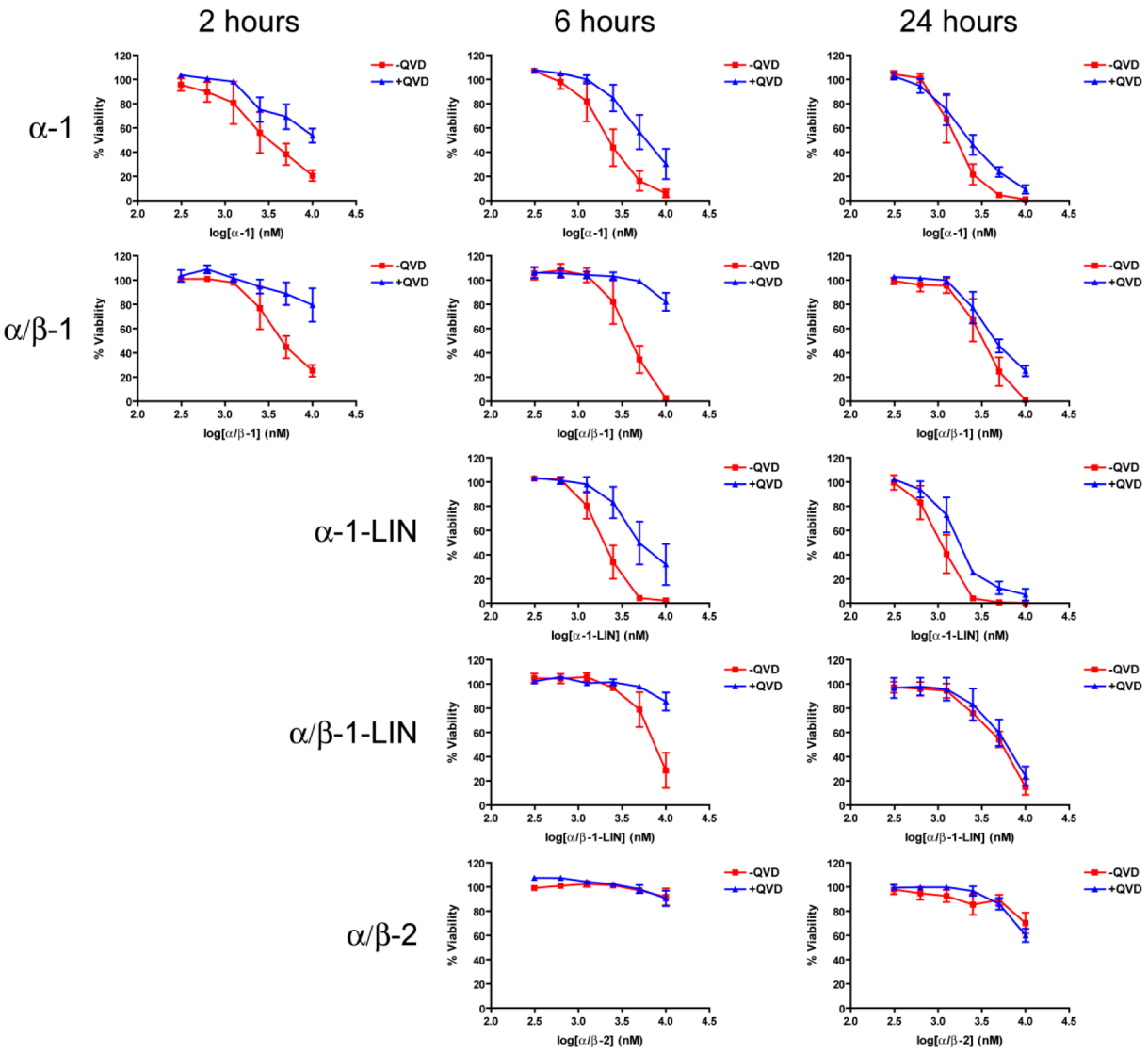

Figure 6. Viability of U937 cells (relative to DMSO control) when treated with various concentrations of α- or α/β-peptides in the absence (red) or presence (blue) of 50 μM caspase inhibitor Q-VD-OPh (QVD), as determined by CellTiter-Glo assay. Cells were treated with the indicated α- or α/β-peptide for 2 h under serum-free conditions, followed by the addition of serum-containing medium and additional incubation until the indicated time point. Each data point represents the mean ± SEM for 3−5 replicate measurements.

report using ***α*-1-LIN**,[31] both linear oligomers were effective at reducing U937 cell viability in a caspase-dependent manner (Figure 6). Indeed, at the 6 h time point there was no statistically significant difference in the killing activity of the linear versus the cyclized peptides. In contrast, the α/β-peptide that contained ACPC residues in place of the hydrocarbon cross-link (***α*/*β*-2**) had no significant effect on cell viability, even after 24 h.

We next used another marker of apoptosis, propidium iodide (PI) staining of DNA as detected by fluorescence microscopy, to monitor cell viability and morphology over time (Figure 7). U937 cells were treated with 5 μM of ***α*/*β*-1** or ***α*-1** and imaged every 30 min. The results closely matched the CellTiter-Glo assay data, although cell killing appeared to proceed with slightly different kinetics, presumably due to the differences in experimental read-out between the two assays. These studies revealed a dependence on caspase activity for cell killing by both ***α*/*β*-1** and ***α*-1**, particularly at the earlier time points, as indicated by the delay in cell death for conditions containing Q-VD-OPh (Figure 7A). These observations are fully consistent with those based on CellTiter-Glo assays. Close examination of the images reveals that even after just 1 h of treatment, classical features of apoptotic cell death such as membrane blebbing start to appear. These features are present in the majority of cells within 2 h (Figure 7B), but are not seen in the presence of caspase inhibitor Q-VD-OPh. Significant PI staining (i.e., to >50% of cells) was slightly delayed in cells treated with ***α*/*β*-1** compared to ***α*-1**, consistent with the CellTiter-Glo results, suggesting ***α*-1** killed more rapidly than did ***α*/*β*-1** (Figure 7A). The majority of cells treated with either ***α*/*β*-1** or ***α*-1**, however, were dead (PI^{+ve}) within 2−6 h, and this cell death was accompanied by the prodigious release of small apoptotic bodies, another hallmark of apoptosis induction.

Cytochrome *c* Release Assay (Unpermeabilized U937 Cells). To further assess whether cell killing by stapled ***α*/*β*-1** occurred via the mitochondrial pathway, we examined unpermeabilized U937 cells for cytochrome *c* release 3 h after treatment (Figure 8). Here we observed that most of the cytochrome *c* was present in the soluble fraction, which contrasted with the location of cytochrome *c* exclusively in the

DOI: 10.1021/jacs.5b05896
J. Am. Chem. Soc. 2015, 137, 11365−11375

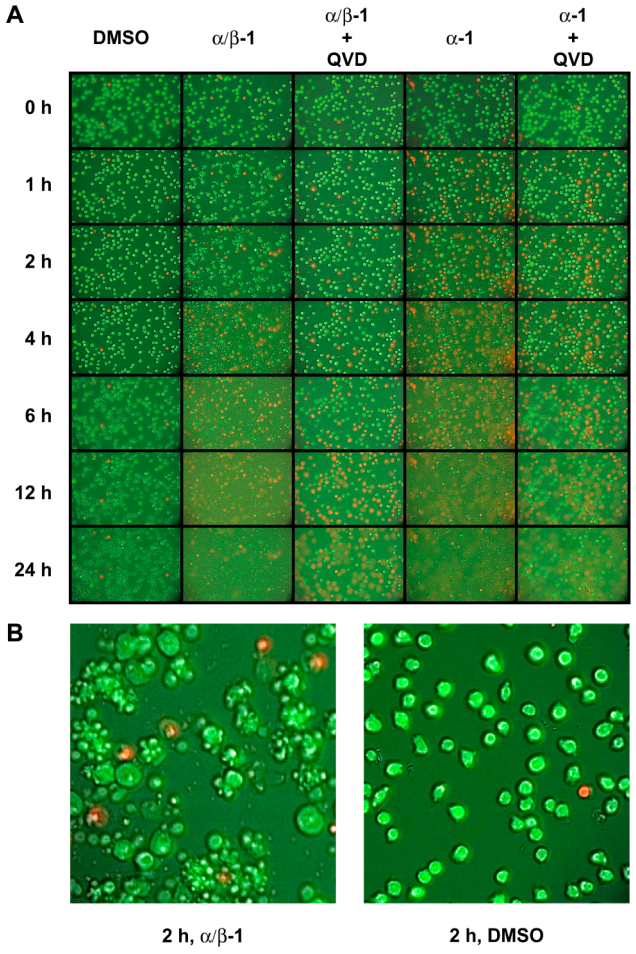

Figure 7. (A) Analysis of U937 cell killing over time induced by 5 μM ***α*/*β*-1** or ***α*-1** in the absence or presence of 50 μM Q-VD-OPh (QVD). Green cells indicate those stained for CellTracker Green dye (living cells). Red cells indicate cells stained by PI (dead cells). (B) Close up of the indicated conditions from panel A, highlighting morphological changes resulting from treatment with ***α*/*β*-1** relative to DMSO control.

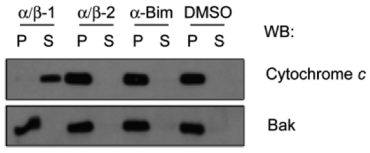

Figure 8. Cytochrome *c* release assay on unpermeabilized U937 cells treated with 10 μM of the indicated α- or α/β-peptide for 3 h. ***α*/*β*-1**, but not ***α*/*β*-2** or ***α*-Bim**, was able to induce cytochrome *c* release from the mitochondria-containing pellet fraction (P) to the soluble cytosolic fraction (S). The lower panel indicates Western blot for Bak as a control for membrane permeabilization.

pellet after intact cells were treated with either ***α*-Bim** or ***α*/*β*-2**, neither of which is stapled. The absolute amount of cytochrome *c* detected in cells treated with ***α*/*β*-1** was somewhat lower than the amount in cells subjected to the other treatments; this trend may reflect some degree of leakage through the plasma membrane of the dying cells after treatment with ***α*/*β*-1**.

Cellular Uptake of Fluorescein-Labeled Analogues by Live-Cell Confocal Microscopy. We examined the cellular uptake of fluorescein (Flu)-labeled derivatives of ***α*-Bim, *α*-1, *α*/*β*-1, *α*-1-LIN**, and ***α*/*β*-1-LIN** in both U937 and MEF cells by live-cell confocal microscopy (Figures 9, 10, S4, and S5). When U937 cells were treated with Flu-labeled peptides at 2 μM for 3 h under serum-free conditions, we observed intracellular green fluorescence for both **Flu-*α*-1** and **Flu-*α*/*β*-1** (Figure 9), consistent with the hypothesis that ***α*-1** and ***α*/*β*-1** can cross membranes spontaneously and gain access to targets within the cytoplasm of living cells. We observed similar intracellular fluorescence for **Flu-*α*-1-LIN** and **Flu-*α*/*β*-1-LIN**, which is consistent with our finding that both ***α*-1-LIN** and ***α*/*β*-1-LIN** can also initiate apoptosis in U937 cells. With all oligomers containing the S5 residue, whether subjected to cyclization or not, we also observed significant green fluorescence associated with the outer membrane of some cells, which we interpret as aggregated peptide. These aggregates remained strongly associated with the cell membrane even after multiple washes prior to imaging. U937 cells treated with **Flu-*α*-Bim**, which does not contain the S5 residue, displayed negligible green fluorescence inside cells or associated with the outer membrane, consistent with the hypothesis that ***α*-Bim** does not enter cells.

When MEFs were treated with fluorescein-labeled analogues of Bim-based oligomers, the confocal microscopy images were similar to those seen with the U937 cells, with **Flu-*α*-1**, **Flu-*α*/*β*-1**, **Flu-*α*-1-LIN**, and **Flu-*α*/*β*-1-LIN** all appearing to enter the MEFs (Figure 10). These observations are consistent with a previous report showing that labeled ***α*-1** can enter MEFs, despite the stapled peptide's inability to kill these cells.[16] However, the fluorescent staining pattern appeared somewhat more punctate in the MEFs than was observed with the U937 cells. This result suggests that although the stapled and unstapled α- and α/β-peptides can enter MEFs, these peptides may be unable to move into the cytoplasm in this cell type, in contrast to U937 cells.

Protease Susceptibility. We evaluated a subset of the peptides for susceptibility to degradation by proteinase K, a generic and aggressive protease (Table 1, Figure S1). In this assay, the linear α-peptide ***α*-Bim** was very rapidly degraded, showing a half-life of 0.27 min. ***α*-1**, an α-peptide that contains the hydrocarbon cross-link, showed modestly diminished susceptibility to degradation by proteinase K, with a half-life of 1.6 min under the assay conditions. The ~6-fold increase in half-life for ***α*-1** relative to ***α*-Bim** is consistent with previous reports in terms of the extent to which a hydrocarbon cross-link confers resistance to proteolytic destruction.[23,33] This modest resistance to proteolysis presumably arises from the presence of the α,α-disubstituted residues and the cross-linking segment, both of which favor a helical conformation. ***α*/*β*-1**, which contains three cyclic β-amino acid residues in addition to the cross-link, showed a large improvement in resistance to proteolysis relative to ***α*-1**, with a half-life of 150 min (>90-fold increase in relative to the stapled peptide ***α*-1** and >500-fold increase relative to ***α*-Bim**). Thus, the incorporation of β-amino acid residues can be used to develop an α/β-peptide analogue that mimics the complex functions of a stapled α-peptide (apoptosis initiation in certain cell types, in the case of ***α*-1**) while dramatically reducing susceptibility to protease degradation.

DISCUSSION

We have previously shown that properly designed α/β-peptides, in which the peptidic backbone deviates from that of conventional peptides and proteins, are able to mimic analogous α-peptides structurally and functionally in terms of

DOI: 10.1021/jacs.5b05896
J. Am. Chem. Soc. 2015, 137, 11365−11375

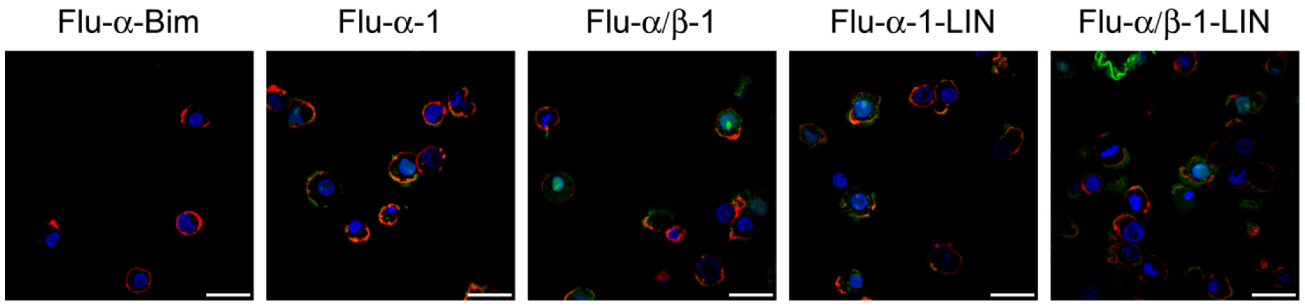

Figure 9. Analysis of U937 cellular uptake of fluorescein (Flu)-labeled analogues of α- and α/β-peptides by live-cell confocal microscopy. Cells were treated with 2 μM of the indicated α- or α/β-peptide in serum-free medium for 3 h prior to imaging. Images were obtained under 90× magnification, showing the channels for green (fluorescein, peptide), red (WGA488, outer membrane stain), and blue (Hoescht 33342, nuclear stain). Scale bars represent 25 μm.

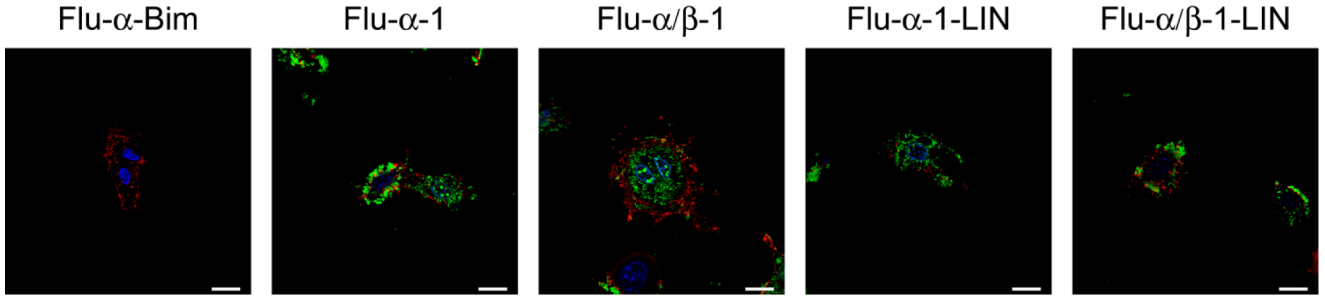

Figure 10. Analysis of MEF cellular uptake of fluorescein (Flu)-labeled analogues of α- and α/β-peptides by live-cell confocal microscopy. Cells were treated with 2 μM of the indicated α- or α/β-peptide in serum-free medium for 3 h prior to imaging. Images were obtained under 60× magnification, showing the channels for green (fluorescein, peptide), red (WGA488, outer membrane stain), and blue (Hoescht 33342, nuclear stain). Scale bars represent 25 μm.

selective recognition of target proteins *in vitro*.[3,4,7] Furthermore, recent studies have shown that α/β-peptides can exhibit improved properties *in vivo* relative to analogous α-peptides, likely due to a decreased susceptibility of the unnatural α/β backbone to proteolytic destruction.[8] However, the inability of most α- and α/β-peptides to cross cellular membranes has limited these compounds to extracellular targets for cellular and *in vivo* applications. The remarkable ability of the so-called "stapled" BH3 domain peptides (first reported by Walensky et al.) to penetrate cell membranes and initiate apoptosis[16,23] led us to investigate whether α/β-peptide analogues of a hydrocarbon-cross-linked BH3 α-peptide could retain these interesting and useful characteristics.

Several reports have highlighted the large impact of primary sequence on the activity of stapled α-peptides in living cells. Small changes in sequence or charge can significantly alter the ability of these peptides to enter cells, which indicates that the presence of a hydrocarbon cross-linker does not ensure membrane transit.[19,24,34] In light of these results, it was of interest to determine whether the replacement of a subset of α-amino acid residues with β-amino acid residues in a known, active cell-penetrating stapled peptide (**α-1**, often referred to in prior reports as **BimSAHB**[15,16]) would alter the ability of the resulting α/β-peptides to cross cell membranes and initiate apoptosis.

To evaluate the impact of $\alpha \rightarrow \beta$-residue substitution on the activity of the α-peptide **α-1**, we designed **α/β-1** using an $\alpha \rightarrow \beta$ substitution pattern previously shown to be effective for mimicry of the Bim BH3 domain.[11] **α/β-1**, along with linear analogue **α/β-1-LIN** and an analogue bearing ACPC residues in place of the S5 residues (**α/β-2**), were able to bind tightly to anti-apoptotic proteins (Table 1), indicating that the $\alpha \rightarrow \beta$ substitutions did not dramatically alter protein recognition (although **α/β-2** displayed reduced affinity for Bcl-x_L and Bcl-2 relative to **α/β-1** and **α/β-1-LIN**). **α/β-1** and **α/β-2** both displayed activity similar to that of the prototype α-peptide **α-Bim** in promoting Bax/Bak-dependent cytochrome *c* release in membrane-permeabilized MEFs (Figure 4), indicating that each of these α/β-peptides can engage the apoptotic machinery in a cellular environment if the membrane barrier is removed.

The crystal structures of **α/β-1** and **α/β-1-LIN** bound to Bcl-2 demonstrate that these α/β-peptides engage the BH3-recognition groove of the anti-apoptotic protein, making all of the expected side chain contacts to Bcl-2 (Figure 3). Overall, the co-crystal structures indicate that both **α/β-1** and **α/β-1-LIN** recapitulate the classic BH3 binding mode and that incorporation of the S5 and cyclic β-amino acid residues does not dramatically alter the structure or binding mode of the resulting α/β-peptides relative to that of a classical α-helical BH3 domain. To our knowledge, these are the first crystal structures of α/β-peptides containing the recently reported cyclic β-amino acid residue sAPC[11] and the first structures of an α/β-peptide bound to Bcl-2.

When tested against a broad panel of noncancerous and cancerous cell lines, **α/β-1** showed the same profile of activity as **α-1**, efficiently killing U937 lymphoma cells while having negligible impact on the viability of the other cell lines tested (Figure 5). This very selective activity is consistent with the previous reports of **α-1**[16,31] and may be due to the high reliance on Mcl-1 for survival that is characteristic of acute myeloid leukemia cells such as U937.[35] Both **α/β-1** and **α-1** bind to Mcl-1 with high affinity (Table 1). Live-cell confocal microscopy indicated that fluorescein-labeled analogues of **α/β-1**, **α/β-1-LIN**, and **α-1-LIN** were each able to enter U937

DOI: 10.1021/jacs.5b05896
J. Am. Chem. Soc. 2015, 137, 11365−11375

cells in a manner similar to the entry of fluorescein-labeled **α-1** (Figures 9, S4, and S5). Our detailed viability studies indicated that the ability of **α/β-1** to kill U937 cells was dose dependent, attenuated by caspase inhibitor Q-VD-OPh, and resulted in significant cell membrane blebbing and release of "apoptotic bodies", all consistent with the induction of apoptosis rather than an off-target cytotoxic effect (Figures 6 and 7). Furthermore, the release of cytochrome *c* from the mitochondria of unpermeabilized U937 cells is consistent with initiation of the apoptotic pathway by **α/β-1** (Figure 8). These data demonstrate that the on-target effects of **α/β-1** are in line with those documented in previous studies showing that stapled BH3 peptides, including **α-1**, are able to initiate apoptosis in certain cell types.[16,23,31] Interestingly, at the 24 h time point, the level of cell death that could be inhibited by Q-VD-OPh was significantly less than at the earlier time points. This observation could indicate that the caspase inhibitor was "overwhelmed" due to the sustained apoptosis activation in the cells. An alternative explanation is that prolonged exposure of cells to the stapled peptides (or nonstapled but S5-containing peptides) results in nonspecific toxicity. This latter hypothesis is consistent with a recent report[36] showing that stapled helical α-peptides based on the N-terminal segment of p53 kill cells in a p53-independent manner because these peptides cause disruption of the plasma membrane, which leads to nonspecific cell death at high peptide concentrations (>10 μM). Further studies would be required to establish whether either of these explanations accounts for the apparent noncaspase-dependent death after long-term exposure of U937 cells to the peptides discussed here.

Neither **α-1** nor **α/β-1** demonstrated any significant killing activity toward MEFs, an observation that is consistent with previous reports regarding the effects of stapled BH3 peptides on these cells.[16,19] These results are somewhat surprising given that (1) our binding assays showed that **α/β-1** and **α-1** can bind tightly to both Mcl-1 and Bcl-x_L, the critical anti-apoptotic proteins in MEFs (Table 1), (2) assays using permeabilized cells demonstrated that **α/β-1** can induce cytochrome *c* release in MEFs (Figure 4), and (3) live-cell imaging demonstrated that fluorescein-labeled analogues of both **α-1** and **α/β-1** can enter these cells (Figure 10). One explanation for this lack of activity could be that the peptides do not reach the cytoplasm of MEF cells and instead remain trapped within intracellular vesicles. This possibility is consistent with the punctate staining pattern revealed by our live-cell imaging of MEF cells. However, it is unclear why these peptides are able to enter the cytoplasm of U937 cells; the unique features that allow U937 cytoplasm entry merit further investigation. It is also unclear from our study why neither **α-1** nor **α/β-1** caused toxicity toward other cancer cell lines tested (this behavior has been previously noted for **α-1**).[31] One possibility is that the peptides become trapped within vesicles in these cells. A second possibility is that these peptides are not taken up via endocytosis in these cell types. A third possibility is that the peptides do not bind sufficiently tightly to the critical anti-apoptotic protein (e.g., Bcl-2) in these cell types.

Recent reports have highlighted examples of linear ("unstapled") analogues of stapled α-peptides that contain the S5 residue and manifest cell-killing activity.[31,32] The experiments reported here are consistent with these precedents; we observe that the linear α-peptide **α-1-LIN** and the linear α/β-peptide **α/β-1-LIN** are able to enter cells (Figures 9 and 10) and initiate apoptosis in U937 cells (Figure 6). These results, together with the similar IC_{50} values displayed by pairs of stapled and unstapled analogues (i.e., by **α-1** and **α-1-LIN**, and by **α/β-1** and **α/β-1-LIN**) and the co-crystal structures of complexes formed by **α/β-1** or **α/β-1-LIN** with Bcl-2, suggest that the S5 residue is a critical determinant of biochemical and cellular activity, whether or not a covalent cross-link is formed. The role of this α,α-disubstituted α-amino acid residue could arise from the high intrinsic hydrophobicity and/or from the strong helix-promoting properties that are well-known for residues of this type, such as 2-aminoisobutyric acid (Aib). Indeed, our CD data (Figure 2) show that the presence of two S5 residues leads to a significant enhancement in α-peptide helicity, even in the absence of a cross-link. The lack of cellular activity for **α/β-2**, which does not contain S5 residues, raises the possibility that some aspect of the α,α-disubstituted unit is important for cell entry. However, an alternative explanation for the lack of **α/β-2** activity is the low affinity of this α/β-peptide for some anti-apoptotic proteins (Table 1), which is also reflected in this α/β-peptide's decreased ability to induce cytochrome *c* release in permeabilized MEFs relative to **α/β-1** (Figure 4).

One major motivation for the design of α/β-peptide analogues of α-helical α-peptides is to decrease susceptibility to proteolysis. Stapled α-helical α-peptides containing two S5 residues cross-linked by olefin metathesis are less prone to protease degradation relative to analogous nonstapled α-peptides containing only natural residues, presumably because of enhanced helicity conferred by introduction of the α,α-disubstituted S5 residues and the covalent cross-link.[22−24] The data presented here show that incorporating a small number of β-amino acid residues into the stapled α-peptide **α-1** (to generate **α/β-1**) leads to a much more pronounced protection from proteolysis than does introduction of the S5 α-residues and the staple alone (Table 1). Overall, cross-linked α/β-peptides may be better suited for eventual *in vivo* applications than are cross-linked α-peptides. One caveat to these studies is that the incorporation of the S5 residue appears to result in a tendency for both α- and α/β-peptides to aggregate, as judged by CD experiments. This conclusion is consistent with previous reports on α-peptides containing S5 residues.[37] Susceptibility to proteolysis is likely to be influenced by staple incorporation, by β-residue incorporation, and by aggregation, and it is not possible from our data to isolate the effect exerted by each of these factors. Nevertheless, the increase in protease resistance we observed for **α/β-1** versus **α-1** is consistent with many prior reports from our groups involving α → β substitutions.[3−7,10,11] Other significant limitations of the stapling strategy, which we observed both for α-peptides and α/β-peptides, including low aqueous solubility, inactivation in the presence of serum (Figure S6), and activity toward only limited cell types, remain to be addressed.[24]

■ CONCLUSIONS

We have described the design of an α/β-peptide analogue of a "stapled" α-helical α-peptide that structurally and functionally mimics the original stapled α-peptide and can kill one type of cancer cell by engaging anti-apoptotic protein targets. This report marks the first demonstration that an intracellular protein−protein interaction can be modulated by an α/β-peptide. Because α/β-peptides are less susceptible to proteolytic degradation than are their α-peptide analogues, stapled α/β-peptides may be useful for probing the functional roles of specific protein−protein interactions in living cells.

DOI: 10.1021/jacs.5b05896
J. Am. Chem. Soc. 2015, 137, 11365−11375

Ultimately such α/β-peptides might serve as starting points for the development of therapeutic agents. The results presented here show that backbone modification via periodic $\alpha \rightarrow \beta$-residue replacement can deliver oligomers that are highly resistant to proteolysis while retaining other desirable properties of the original α-peptide, particularly cell-permeability and specific protein recognition.

EXPERIMENTAL METHODS

Peptide and α/β-peptide Synthesis and Purification. α-Peptides and α/β-peptides were synthesized by microwave-assisted solid-phase peptide synthesis on NovaPEG Rink Amide resin, as previously described.[38] Full details on peptide labeling, the metathesis reaction, and purification can be found in the Supporting Information.

Recombinant Protein Expression and Purification. Recombinant Bcl-2 anti-apoptotic proteins with N- and/or C-terminal truncations for binding studies (Bcl-2ΔC22, Bcl-x_LΔC24, Mcl-1ΔN170ΔC23) were expressed and purified as described previously for hexahistidine tagged proteins (in the case of Bcl-2)[39] or GST tagged proteins (in the case of Bcl-x_L and Mcl-1).[28] The human Bcl-2 construct (Bcl-2ΔC32ΔLoop) used for crystallization was identical to that reported previously for structural studies.[40] This construct has the large unstructured loop between residues 35−91 replaced with residues 35−50 of Bcl-x_L. The C-terminal 32 residues corresponding to the hydrophobic transmembrane domain were also deleted to improve protein solubility. The protein was expressed as a GST fusion protein from a pGEX6P3 vector and purified using glutathione-affinity chromatography followed by gel-filtration chromatography.

Surface Plasmon Resonance. Solution competition assays were performed using a Biacore 3000 instrument exactly as described previously.[41]

Circular Dichroism (CD). CD measurements were carried out in purified water using an Aviv Model 420 circular dichroism spectrometer. Spectra were collected in a quartz cuvette (0.1 or 1 cm) at 20 °C with a wavelength step size of 1 nm and a 10 s averaging time.

Crystallography. Crystals were obtained by mixing Bcl-2ΔC32ΔLoop with each peptide at a molar ratio of 1:1.3 and then concentrating the sample to 10 mg/mL. Crystallization trials were performed at the Bio21 Collaborative Crystallization Centre. All crystals were grown by the sitting drop method at room temperature. For the ***α/β*-1**:Bcl-2 structure, the crystals were grown in 20 mM $CaCl_2$, 0.1 M sodium MOPS pH 7.0, 10% (v/v) 2-propanol. For the ***α/β*-1-LIN**:Bcl-2 structure, the crystals were grown in 0.1 M $CaCl_2$, 0.1 M MES pH 6.5, 20% (v/v) ethanol. Prior to cryo-cooling in liquid N_2, crystals were equilibrated into cryoprotectant consisting of reservoir solution containing 15% (v/v) ethylene glycol. Crystals were mounted directly from the drop and plunge-cooled in liquid N_2.

Crystal Diffraction Data Collection and Structure Determination. Diffraction data were collected at 100 K at the Australian Synchrotron MX2 beamline (Victoria, Australia) (wavelength for both structures was 0.9537 Å). The diffraction data were integrated and scaled with XDS.[42] The structure was obtained by molecular replacement with PHASER[43] using the crystal structure of the Bcl-2:Bax BH3 complex (PDB code 2XA0)[29] with the BH3 peptide removed as the search model. Multiple rounds of building in COOT[44] and refinement in PHENIX[45] led to the final model.

Cytochrome *c* Release Assays. Cytochrome *c* release assays with digitonin-permeabilized MEFs were performed as described previously.[41] For the cytochrome *c* release assay with the unpermeabilized U937 cells, 2×10^6 cells were treated with peptides (10 μM) for 3 h at 37 °C before pelleting by centrifugation. Cell pellets were then resuspended in digitonin-containing lysis buffer (20 mM HEPES pH 7.2, 100 mM KCl, 5 mM $MgCl_2$, 1 mM EDTA, 1 mM EGTA, 250 mM sucrose, 0.05% (w/v) digitonin (Calbiochem) supplemented with protease inhibitors (Roche)) for 45 min at 30 °C to permeabilize the plasma membrane, then pelleted again. The supernatant was retained (soluble fraction), and the pellet resuspended in cell-lysis buffer (20 mM Tris pH 7.4, 135 mM NaCl, 1.5 mM $MgCl_2$, 1 mM EDTA, 1% (v/v) Triton X-100, 10% (v/v) glycerol supplemented with protease inhibitors (Roche)) and incubated on ice for 1 h before centrifugation. This supernatant was then retained as the pellet fraction. Both soluble and pellet fractions were subsequently analyzed by Western blotting using an anticytochrome *c* antibody (clone 7H8.2C12; BD Biosciences).

Cell Killing Assay. U937 and adherent cancer cells (MDA-MB-231, MDA-MB-468, LIM-2405, SW480, and A549) were maintained in RPMI medium supplemented with 10% (v/v) fetal bovine serum (FBS). MEFs were maintained in FMA medium (DME KELSO medium supplemented with 10% (v/v) FBS, 250 μM L-asparagine and 50 μM 2-mercaptoethanol). Cell killing assays were performed similarly to those described previously for testing stapled peptides.[16] U937 cells were aliquoted (1×10^4 cells in 50 μL) into 96-well opaque plates and incubated with serial dilutions of peptides or DMSO (± 50 μM Q-VD-OPh) in serum-free RPMI medium for 2 h, followed by addition of 50 μL RPMI containing 20% FBS (final concentration FBS 10% (v/v) in 100 μL). Cells were incubated for a further 0, 4, or 22 h prior to addition of CellTiter-Glo chemiluminescence reagent (for a total time of 2, 6, or 24 h incubation with peptide), and luminescence measured on Lumistar Optima (BMG Labtech) microplate reader. For assays using adherent cells, cells were plated in their respective media described above (1.5×10^3 cells/well), then 24 h later were washed with the corresponding serum-free medium prior to addition and incubation with the peptides or DMSO, as for the U937 cells.

Analysis of Cell Killing by Live-Cell Imaging. U937 cells were plated in a black 96-well optical bottom plate (5×10^4 cells/well) together with DMSO, peptides (5 μM) ± Q-VD-OPh (50 μM) in phenol-red and serum-free RPMI medium (final volume 100 μL) containing CellTracker Green dye (Life Technologies, C2925), and PI (2 μg/mL). Cells were imaged every 30 min for 24 h on a Zeiss Live Cell Observer, consisting of an Axiovert 200 M inverted microscope, equipped with environmental control and CO_2, LED Colibri illumination, a 20×/0.8 NA objective and AxioCam MRm camera. Zeiss filter set Ex 470/40 and Em 525/50 together with LED module 470 was used for CellTracker Green fluorescence and Ex 560/40 and 630/75 together with LED module 540−580 for PI fluorescence.

Analysis of Cellular Uptake by Live-Cell Confocal Microscopy. After treatment under the conditions indicated in the figures, U937s and MEFs were washed and then imaged using an inverted Eclipse Ti-E A1R-Si laser scanning confocal microscope (Nikon) equipped with Plan Apo 10× DIC L, Plan Apo VC 20× DIC N2, and Plan Apo VC 60× Oil DIC N2 objectives, a 1.5× optical zoom, lasers for 405 nm (blue), 488 nm (green), and 561/594 nm (red) wavelengths, a dichroic mirror (405/488/561/640), filters for 450/50, 525/50, and 595/50 nm wavelengths, a galvano scanning head, and a computer running NIS Elements software. U937 cells were imaged at 10× and at 60× (with 1.5× magnifier) with lasers for blue, green, and red. MEFs were imaged at 60× with lasers for blue, green, and red. Images were collected using 4× averaging, 6.4 ms dwell, and 1024 × 1024 image size. Images were brightness-adjusted uniformly across conditions at a given magnification using NIS Elements v4.1 software (Nikon).

Protease Susceptibility Assay. Stock solutions of ∼100 μM peptide or α/β-peptide in water with 10% DMSO (for solubility) were prepared, as determined by UV absorbance at 280 nm.[46] Solutions were then diluted in 10% DMSO/water to 50 μM, and a solution of 50 μg/mL proteinase K in TBS (50 mM Tris pH 7.5, 200 mM NaCl) was added to give final concentrations = 40 μM peptide, 10 μg/mL proteinase K in 10 mM Tris, 40 mM NaCl, 8% DMSO. Protease reactions were allowed to proceed at room temperature, and each reaction was run in duplicate. At each time point, 50 μL of the reaction solution was quenched with 125 μL of 1:1 water/acetonitrile + 1% trifluoroacetic acid. The resulting quenched solution (125 μL) was injected onto analytical HPLC. The amount of relative remaining oligomer at each time point was determined by integration of the peak at 220 nm in the resulting chromatogram. Half-lives were determined by plotting the amount of peptide remaining versus reaction time and fitting the data to an exponential decay model in GraphPad Prism 4.0 (Figure S1).

DOI: 10.1021/jacs.5b05896
J. Am. Chem. Soc. 2015, 137, 11365−11375

■ ASSOCIATED CONTENT

Supporting Information

The Supporting Information is available free of charge on the ACS Publications website at DOI: 10.1021/jacs.5b05896.

Additional details for experimental protocols, Figures S1−S7, and Table S1 (PDF)

■ AUTHOR INFORMATION

Corresponding Authors

*gellman@chem.wisc.edu

*doug.fairlie@onjcri.org.au

Present Address

#Olivia Newton-John Cancer Research Institute, Heidelberg, Victoria, 3084, Australia; School of Cancer Medicine, La Trobe University, Melbourne, Victoria, 3084, Australia; Department of Chemistry and Physics, La Trobe Institute of Molecular Science, Melbourne, Victoria, 3086, Australia

Notes

The authors declare the following competing financial interest(s): S.H.G. is a cofounder of Longevity Biotech, Inc., which is pursuing biomedical applications of α/β-peptides.

■ ACKNOWLEDGMENTS

This research was supported by NIGMS (GM056414, to S.H.G.) and grants and fellowships from the NHMRC of Australia (Project Grant 1041936, to W.D.F., and Career Development Fellowship 1024620, to E.F.L.) and Cancer Council Victoria (Grant-in-aid 1057949). Infrastructure support from NHMRC IRIISS grant no. 361646 and the Victorian State Government OIS grant is gratefully acknowledged. J.W.C. was supported in part by a Biotechnology Training Grant (NIH Grant T32 GM008349). Additional support was provided by NIH (HL093282, to W.L.M., and GM044783, to R.T.R.). In addition, W.L.M. acknowledges support from the University of Wisconsin−Madison Nanoscale Science and Engineering Center (DMR-0832760).

■ REFERENCES

(1) (a) Wells, J. A.; McClendon, C. L. *Nature* **2007**, *450*, 1001−1009. (b) Arkin, M. R.; Tang, Y.; Wells, J. A. *Chem. Biol.* **2014**, *21*, 1102−1114.

(2) Vlieghe, P.; Lisowski, V.; Martinez, J.; Khrestchatisky, M. *Drug Discovery Today* **2010**, *15*, 40−56.

(3) Horne, W. S.; Boersma, M. D.; Windsor, M. A.; Gellman, S. H. *Angew. Chem., Int. Ed.* **2008**, *47*, 2853−2856.

(4) Horne, W. S.; Johnson, L. M.; Ketas, T. J.; Klasse, P. J.; Lu, M.; Moore, J. P.; Gellman, S. H. *Proc. Natl. Acad. Sci. U. S. A.* **2009**, *106*, 14751−14756.

(5) Johnson, L. M.; Gellman, S. H. *Methods Enzymol.* **2013**, *523*, 407−429.

(6) Haase, H. S.; Peterson-Kaufman, K. J.; Levengood, S. K. L.; Checco, J. W.; Murphy, W. L.; Gellman, S. H. *J. Am. Chem. Soc.* **2012**, *134*, 7652−7655.

(7) Checco, J. W.; Kreitler, D. F.; Thomas, N. C.; Belair, D. G.; Rettko, N. J.; Murphy, W. L.; Forest, K. T.; Gellman, S. H. *Proc. Natl. Acad. Sci. U. S. A.* **2015**, *112*, 4552−4557.

(8) (a) Cheloha, R. W.; Maeda, A.; Dean, T.; Gardella, T. J.; Gellman, S. H. *Nat. Biotechnol.* **2014**, *32*, 653−655. (b) Johnson, L. M.; Barrick, S.; Hager, M. V.; McFedries, A.; Homan, E. A.; Rabaglia, M. E.; Keller, M. P.; Attie, A. D.; Saghatelian, A.; Bisello, A.; Gellman, S. H. *J. Am. Chem. Soc.* **2014**, *136*, 12848−12851.

(9) (a) Jochim, A. L.; Arora, P. S. *Mol. BioSyst.* **2009**, *5*, 924−926. (b) Jochim, A. L.; Arora, P. S. *ACS Chem. Biol.* **2010**, *5*, 919−923.

(10) Boersma, M. D.; Haase, H. S.; Peterson-Kaufman, K. J.; Lee, E. F.; Clarke, O. B.; Colman, P. M.; Smith, B. J.; Horne, W. S.; Fairlie, W. D.; Gellman, S. H. *J. Am. Chem. Soc.* **2012**, *134*, 315−323.

(11) Peterson-Kaufman, K. J.; Haase, H. S.; Boersma, M. D.; Lee, E. F.; Fairlie, W. D.; Gellman, S. H. *ACS Chem. Biol.* **2015**, *10*, 1667−1675.

(12) (a) Gross, A.; McDonnell, J. M.; Korsmeyer, S. J. *Genes Dev.* **1999**, *13*, 1899−1911. (b) Cory, S.; Huang, D. C. S.; Adams, J. M. *Oncogene* **2003**, *22*, 8590−8607. (c) Willis, S. N.; Fletcher, J. I.; Kaufmann, T.; van Delft, M. F.; Chen, L.; Czabotar, P. E.; Ierino, H.; Lee, E. F.; Fairlie, W. D.; Bouillet, P.; Strasser, A.; Kluck, R. M.; Adams, J. M.; Huang, D. C. S. *Science* **2007**, *315*, 856−859.

(13) (a) Oltersdorf, T.; Elmore, S. W.; Shoemaker, A. R.; Armstrong, R. C.; Augeri, D. J.; Belli, B. A.; Bruncko, M.; Deckwerth, T. L.; Dinges, J.; Hajduk, P. J.; Joseph, M. K.; Kitada, S.; Korsmeyer, S. J.; Kunzer, A. R.; Letai, A.; Li, C.; Mitten, M. J.; Nettesheim, D. G.; Ng, S.; Nimmer, P. M.; O'Connor, J. M.; Oleksijew, A.; Petros, A. M.; Reed, J. C.; Shen, W.; Tahir, S. K.; Thompson, C. B.; Tomaselli, K. J.; Wang, B.; Wendt, M. D.; Zhang, H.; Fesik, S. W.; Rosenberg, S. H. *Nature* **2005**, *435*, 677−681. (b) Lessene, G.; Czabotar, P. E.; Colman, P. M. *Nat. Rev. Drug Discovery* **2008**, *7*, 989−1000.

(14) (a) Rudin, C. M.; Hann, C. L.; Garon, E. B.; de Oliveira, M. R.; Bonomi, P. D.; Camidge, D. R.; Chu, Q.; Giaccone, G.; Khaira, D.; Ramalingam, S. S.; Ranson, M. R.; Dive, C.; McKeegan, E. M.; Chyla, B. J.; Dowell, B. L.; Chakravartty, A.; Nolan, C. E.; Rudersdorf, N.; Busman, T. A.; Mabry, M. H.; Krivoshik, A. P.; Humerickhouse, R. A.; Shapiro, G. I.; Gandhi, L. *Clin. Cancer Res.* **2012**, *18*, 3163−3169. (b) Pan, R.; Hogdal, L. J.; Benito, J. M.; Bucci, D.; Han, L.; Borthakur, G.; Cortes, J.; DeAngelo, D. J.; Debose, L.; Mu, H.; Dohner, H.; Gaidzik, V. I.; Galinsky, I.; Golfman, L. S.; Haferlach, T.; Harutyunyan, K. G.; Hu, J.; Leverson, J. D.; Marcucci, G.; Muschen, M.; Newman, R.; Park, E.; Ruvolo, P. P.; Ruvolo, V.; Ryan, J.; Schindela, S.; Zweidler-McKay, P.; Stone, R. M.; Kantarjian, H.; Andreeff, M.; Konopleva, M.; Letai, A. G. *Cancer Discovery* **2014**, *4*, 362−375.

(15) Walensky, L. D.; Pitter, K.; Morash, J.; Oh, K. J.; Barbuto, S.; Fisher, J.; Smith, E.; Verdine, G. L.; Korsmeyer, S. J. *Mol. Cell* **2006**, *24*, 199−210.

(16) LaBelle, J. L.; Katz, S. G.; Bird, G. H.; Gavathiotis, E.; Stewart, M. L.; Lawrence, C.; Fisher, J. K.; Godes, M.; Pitter, K.; Kung, A. L.; Walensky, L. D. *J. Clin. Invest.* **2012**, *122*, 2018−2031.

(17) Lau, Y. H.; de Andrade, P.; Wu, Y.; Spring, D. R. *Chem. Soc. Rev.* **2015**, *44*, 91−102.

(18) (a) Felix, A. M.; Heimer, E. P.; Wang, C. T.; Lambros, T. J.; Fournier, A.; Mowles, T. F.; Maines, S.; Campbell, R. M.; Wegrzynski, B. B.; Toome, V.; Fry, D.; Madison, V. S. *Int. J. Pept. Protein Res.* **1988**, *32*, 441−454. (b) Murage, E. N.; Gao, G.; Bisello, A.; Ahn, J. M. *J. Med. Chem.* **2010**, *53*, 6412−6420.

(19) Okamoto, T.; Zobel, K.; Fedorova, A.; Quan, C.; Yang, H.; Fairbrother, W. J.; Huang, D. C. S.; Smith, B. J.; Deshayes, K.; Czabotar, P. E. *ACS Chem. Biol.* **2013**, *8*, 297−302.

(20) Jo, H.; Meinhardt, N.; Wu, Y.; Kulkarni, S.; Hu, X.; Low, K. E.; Davies, P. L.; DeGrado, W. F.; Greenbaum, D. C. *J. Am. Chem. Soc.* **2012**, *134*, 17704−17713.

(21) (a) Blackwell, H. E.; Grubbs, R. H. *Angew. Chem., Int. Ed.* **1998**, *37*, 3281−3284. (b) Blackwell, H. E.; Sadowsky, J. D.; Howard, R. J.; Sampson, J. N.; Chao, J. A.; Steinmetz, W. E.; O'Leary, D. J.; Grubbs, R. H. *J. Org. Chem.* **2001**, *66*, 5291−5302. (c) Wang, D.; Liao, W.; Arora, P. S. *Angew. Chem., Int. Ed.* **2005**, *44*, 6525−6529. (d) Patgiri, A.; Joy, S. T.; Arora, P. S. *J. Am. Chem. Soc.* **2012**, *134*, 11495−11502. (e) Bergman, Y. E.; Del Borgo, M. P.; Gopalan, R. D.; Jalal, S.; Unabia, S. E.; Ciampini, M.; Clayton, D. J.; Fletcher, J. M.; Mulder, R. J.; Wilce, J. A.; Aguilar, M.; Perlmutter, P. *Org. Lett.* **2009**, *11*, 4438−4440.

(22) Schafmeister, C. E.; Po, J.; Verdine, G. L. *J. Am. Chem. Soc.* **2000**, *122*, 5891−5892.

(23) Walensky, L. D.; Kung, A. L.; Escher, I.; Malia, T. J.; Barbuto, S.; Wright, R. D.; Wagner, G.; Verdine, G. L.; Korsmeyer, S. J. *Science* **2004**, *305*, 1466−1470.

(24) (a) Walensky, L. D.; Bird, G. H. *J. Med. Chem.* **2014**, *57*, 6275−6288. (b) Cromm, P. M.; Spiegal, J.; Grossmann, T. N. *ACS Chem. Biol.* **2015**, *10*, 1362−1375.
(25) Horne, W. S.; Price, J. L.; Keck, J. L.; Gellman, S. H. *J. Am. Chem. Soc.* **2007**, *129*, 4178−4180.
(26) Lee, E. F.; Sadowsky, J. D.; Smith, B. J.; Czabotar, P. E.; Peterson-Kaufman, K. J.; Colman, P. M.; Gellman, S. H.; Fairlie, W. D. *Angew. Chem., Int. Ed.* **2009**, *48*, 4318−4322.
(27) (a) Lee, E. F.; Smith, B. J.; Horne, W. S.; Mayer, K. N.; Evangelista, M.; Colman, P. M.; Gellman, S. H.; Fairlie, W. D. *ChemBioChem* **2011**, *12*, 2025−2032. (b) Sattler, M.; Liang, H.; Nettesheim, D.; Meadows, R. P.; Harlan, J. E.; Eberstadt, M.; Yoon, H. S.; Shuker, S. B.; Chang, B. S.; Minn, A. J.; Thompson, C. B.; Fesik, S. W. *Science* **1997**, *275*, 983−986. (c) Smits, C.; Czabotar, P. E.; Hinds, M. G.; Day, C. L. *Structure* **2008**, *16*, 818−829.
(28) Czabotar, P. E.; Lee, E. F.; van Delft, M. F.; Day, C. L.; Smith, B. J.; Huang, D. C. S.; Fairlie, W. D.; Hinds, M. G.; Colman, P. M. *Proc. Natl. Acad. Sci. U. S. A.* **2007**, *104*, 6217−6222.
(29) Ku, B.; Liang, C.; Jung, J. U.; Oh, B. H. *Cell Res.* **2011**, *21*, 627−641.
(30) Willis, S. N.; Chen, L.; Dewson, G.; Wei, A.; Naik, E.; Fletcher, J. I.; Adams, J. M.; Huang, D. C. S. *Genes Dev.* **2005**, *19*, 1294−1305.
(31) Okamoto, T.; Segal, D.; Zobel, K.; Fedorova, A.; Yang, H.; Fairbrother, W. J.; Huang, D. C. S.; Smith, B. J.; Deshayes, K.; Czabotar, P. E. *ACS Chem. Biol.* **2014**, *9*, 838−839.
(32) Sinclair, J. K. L.; Schepartz, A. *Org. Lett.* **2014**, *16*, 4916−4919.
(33) Bird, G. H.; Madani, N.; Perry, A. F.; Princiotto, A. M.; Supko, J. G.; He, X.; Gavathiotis, E.; Sodroski, J. G.; Walensky, L. D. *Proc. Natl. Acad. Sci. U. S. A.* **2010**, *107*, 14093−14098.
(34) (a) Bernal, F.; Tyler, A. F.; Korsmeyer, S. J.; Walensky, L. D.; Verdine, G. L. *J. Am. Chem. Soc.* **2007**, *129*, 2456−2457. (b) Bird, G. H.; Gavathiotis, E.; LaBelle, J. L.; Katz, S. G.; Walensky, L. D. *ACS Chem. Biol.* **2014**, *9*, 831−837. (c) Bautista, A. D.; Appelbaum, J. S.; Craig, C. J.; Michel, J.; Schepartz, A. *J. Am. Chem. Soc.* **2010**, *132*, 2904−2906.
(35) Glaser, S. P.; Lee, E. F.; Trounson, E.; Bouillet, P.; Wei, A.; Fairlie, W. D.; Izon, D. J.; Zuber, J.; Rappaport, A. R.; Herold, M. J.; Alexander, W. S.; Lowe, S. W.; Robb, L.; Strasser, A. *Genes Dev.* **2012**, *26*, 120−125.
(36) Li, Y. C.; Rodewald, L. W.; Hoppmann, C.; Wong, E. T.; Lebreton, S.; Safar, P.; Patek, M.; Wang, L.; Wertman, K. F.; Wahl, G. M. *Cell Rep.* **2014**, *9*, 1946−1958.
(37) Bhattacharya, S.; Zhang, H.; Cowburn, D.; Debnath, A. K. *Biopolymers* **2012**, *97*, 253−264.
(38) Horne, W. S.; Price, J. L.; Gellman, S. H. *Proc. Natl. Acad. Sci. U. S. A.* **2008**, *105*, 9151−9156.
(39) Lee, E. F.; Dewson, G.; Smith, B. J.; Evangelista, M.; Pettikiriarachchi, A.; Dogovski, C.; Perugini, M. A.; Colman, P. M.; Fairlie, W. D. *Structure* **2011**, *19*, 1467−1476.
(40) Petros, A. M.; Medek, A.; Nettesheim, D. G.; Kim, D. H.; Yoon, H. S.; Swift, K.; Matayoshi, E. D.; Oltersdorf, T.; Fesik, S. W. *Proc. Natl. Acad. Sci. U. S. A.* **2001**, *98*, 3012−3017.
(41) Smith, B. J.; Lee, E. F.; Checco, J. W.; Evangelista, M.; Gellman, S. H.; Fairlie, W. D. *ChemBioChem* **2013**, *14*, 1564−1572.
(42) Kabsch, W. *Acta Crystallogr., Sect. D: Biol. Crystallogr.* **2010**, *66*, 125−132.
(43) (a) McCoy, A. J.; Grosse-Kunstleve, R. W.; Storoni, L. C.; Read, R. J. *Acta Crystallogr., Sect. D: Biol. Crystallogr.* **2005**, *61*, 458−464. (b) Read, R. J. *Acta Crystallogr., Sect. D: Biol. Crystallogr.* **2001**, *57*, 1373−1382. (c) Storoni, L. C.; McCoy, A. J.; Read, R. J. *Acta Crystallogr., Sect. D: Biol. Crystallogr.* **2004**, *60*, 432−438.
(44) Emsley, P.; Cowtan, K. *Acta Crystallogr., Sect. D: Biol. Crystallogr.* **2004**, *60*, 2126−2132.
(45) Adams, P. D.; Grosse-Kunstleve, R. W.; Hung, L. W.; Ioerger, T. R.; McCoy, A. J.; Moriarty, N. W.; Read, R. J.; Sacchettini, J. C.; Sauter, N. K.; Terwilliger, T. C. *Acta Crystallogr., Sect. D: Biol. Crystallogr.* **2002**, *58*, 1948−1954.
(46) Gill, S. C.; Vonhippel, P. H. *Anal. Biochem.* **1989**, *182*, 319−326.

DOI: 10.1021/jacs.5b05896
J. Am. Chem. Soc. 2015, 137, 11365−11375